Anharmonicity of the lowest-frequency A_1(TO) phonon in $PbTiO_3$

C. M. Foster, Z. Li, M. Grimsditch, S.-K. Chan, and D. J. Lam
Materials Science Division, Argonne National Laboratory, 9700 South Cass Avenue, Argonne, Illinois 60439
(Received 29 March 1993)

Detailed Raman studies of the optical phonons in high-quality single-crystal $PbTiO_3$ indicate that the mode energies and symmetry assignments in the literature [G. Burns and B. Scott, Phys. Rev. B 7, 3088 (1973)] must be revised. In this study, all $\mathbf{k}\cong\mathbf{0}$ optical-phonon modes are directly observed and are shown to obey rigorously the Raman selection rules. The angular dependence of the phonon frequencies indicates that the energy of the lowest-frequency A_1(TO) mode is higher than the energy of the lowest-frequency E(LO) mode at 300 K. This indicates that these two $\mathbf{k}\cong\mathbf{0}$ modes will cross at elevated temperature. The A_1(TO) mode exhibits an anomalous line shape, which we attribute to the anharmonic nature of the lattice. The phonon frequencies determine the clamped dielectric constants, $\varepsilon_a(0)$ and $\varepsilon_c(0)$, using the Lydanne-Sachs-Teller relation. These values, when compared to those obtained from impedance measurements, indicate no dielectric dispersion in $PbTiO_3$ between the MHz region and the Raman region.

I. INTRODUCTION

Lead titanate, one of the perovskite ferroelectric (FE) materials, has been extensively studied by a variety of techniques.[1] Experimental studies of the phonon structure in $PbTiO_3$ have been carried out using neutron scattering,[2] infrared absorption,[3] and Raman scattering.[4–7] These results lead to the classification of the ferroelectric phase transition in $PbTiO_3$ as a prototypical example of "soft-mode" displacive behavior. Soft modes were observed in both the paraelectric (PE) and FE phases.[2] Detailed Raman-scattering experiments of $PbTiO_3$ have been carried out by Burns and Scott.[4] These measurements indicated that the line shape of the intense, lowest-frequency E-symmetry transverse-optical (TO) soft mode could be successfully modeled at all temperatures below $T_c\approx 493\,^{\circ}C$ by a damped harmonic-oscillator model with a frequency-independent damping coefficient. However, the lowest-frequency A_1(TO) phonon could not be directly observed. Mean-field as well as self-consistent phonon model calculations[8–10] predict that the frequency of the lowest-energy A_1(TO) mode is proportional to the ferroelectric order parameter in the tetragonal phase. Burns and Scott[4] determined the frequency of this mode by fitting the angular dependence of the oblique phonon spectra (with $\mathbf{k}$ at 45° between the $\mathbf{a}$ and $\mathbf{c}$) axis using Merten's relation.[11] This fit demonstrated the expected soft-mode behavior of the lowest-frequency A_1(TO) phonon. Based on polarization considerations, a more recent Raman study[6] has questioned the frequencies and symmetry assignments of Burns and Scott;[4] however, no explanation was given for the anomalous line shape of the peak associated with the A_1(TO) phonon in Ref. 6 which led Burns and Scott to question the assignment of this feature.

In this paper, we report detailed Raman studies of the optical phonons of high-quality single-crystal $PbTiO_3$. Our results, in agreement with those of Ref. 6, indicate that revisions are needed in the frequency and symmetry assignments of the optical-phonon modes of $PbTiO_3$ established in the literature.[4,5,7] In contrast to all earlier studies, we observed directly all $\mathbf{k}\cong\mathbf{0}$ optical-phonon modes, and demonstrated that the phonons obey rigorously the Raman selection rules. (In this article $\mathbf{k}\cong\mathbf{0}$ should be understood to mean $\mathbf{k}$ small, relative to the Brillouin zone but large enough to lie outside the polariton regime). Mapping of the full angular dependence of the oblique (i.e., off-axis) phonon frequencies indicates that, at 300 K, the energy of the lowest-frequency A_1(TO) mode is higher than the energy of the lowest-frequency E-symmetry longitudinal-optical (LO) mode. Since the A_1(TO) is the soft mode, these two $\mathbf{k}\cong\mathbf{0}$ modes must cross at elevated temperatures. We also observe that the A_1(TO) mode exhibits an anomalous, highly anisotropic line shape which we attribute to the anharmonic nature of the effective interatomic potential associated with this phonon. Using the Lydanne-Sachs-Teller (LST) relation, the Raman frequencies determine the clamped dielectric constants, ε_a and ε_c. These values, when compared to those obtained from impedance measurements, indicate no dielectric dispersion in $PbTiO_3$ between the MHz region and the Raman region ($\approx$4 THz).

II. EXPERIMENT

The $PbTiO_3$ single crystals were grown by a modified flux-solution method.[12] The single crystals consisted of (001) oriented platelets with dimensions of about $3.5\times3.5\times2.0$ mm. Unlike previous studies,[4] the dc resistivity of the as-grown multidomain crystals was very high ($\sim 3.2\times10^{10}\ \Omega\,cm$). Typically, only U^{3+} compensated crystals exhibit such high dc resistivities.[13] The as-grown crystals contained abundant 90° domains which were removed by a piezoelectric detwinning process.[14] The crystals were oriented using Laue backscattering and then mechanically polished to optical quality on all six sides of a parallelepiped. Further 90° domains, which

were induced in the crystals during polishing, were also removed piezoelectrically. The crystals were then subjected to an optimized heat treatment followed by the removal of the crystal's surface layer. We have previously shown that these treatments minimize the low-frequency dielectric dispersion[15] while retaining the high dc resistivity of the crystal ($\sim 1.2\times 10^{10}$ Ω cm). The high dc resistivity allowed electrical polling of the crystals using an electric field of ~ 18 kV/cm at room temperature for 10 min in order to remove 180° domains. This field is greater than the coercive field of $PbTiO_3$ (~ 16.6 kV/cm) reported in the literature.[16] The resulting single crystals were transparent, yellowish in color, and consisted of a single FE domain with final dimensions of $2.5\times 2.5\times 1.5$ mm.

Raman-scattering data were obtained using one of two systems: a Coherent Innova 70 Ar^+ ion laser and a Jobin-Yvon U-1000 double grating monochromator, or a Coherent Innova 90 Ar^+ ion laser and a Spex 1401 double-grating monochromator. Both systems used cooled (-60 °C) RCA C31034A photomultiplier tubes as the detectors in single-channel, photon-counting mode. Samples were mounted in a Hi-Tran gas flow cryostat (for temperature control from 4 to 450 K) with the laser light focused and collected by an achromatic lens. The scattering geometries of the laser light (487.9 nm at 100 nW) were true 180° backscattering, 90° scattering, and platelet.[17] The spectral resolution was ~ 0.5 cm^{-1}. For the selection rule measurements, the incident laser was polarized using a Glan-Taylor calcite prism polarizer and the scattered light was analyzed with a Melles-Griot dichroic sheet polarizer followed by a mica half-wave plate to compensate for the polarization dependence of the monochromator.

III. PHONON MODES AND SYMMETRY ASSIGNMENTS

In the PE phase ($T > T_c$), $PbTiO_3$ is cubic and belongs to the O_h^1 ($Fm3m$) space group with one formula unit per unit cell. At the Γ point in the Brillouin zone, the 12 optical-phonon modes transform as the $3T_{1u}+T_{2u}$ irreducible representation. The T_{1u} modes are infrared active and the T_{2u} mode is silent, neither infrared nor Raman active. Long-range electrostatic forces lift the degeneracy of the T_{1u} modes in the cubic phase into a doubly degenerate T_{1u}(TO) mode (polarization transverse to **k**) and a single T_{1u}(LO) mode (polarization parallel to **k**). This representation of the symmetry of the zone-center phonons is valid only when **k** is along one of the principal directions of the crystal.

In the FE phase ($T < T_c$), $PbTiO_3$ is tetragonal [C_{4v}^1 ($P4mm$) space group], and each T_{1u} mode splits into two modes transforming as A_1+E. The T_{2u} mode splits into two modes transforming as B_1+E. All modes are both Raman and infrared active. As in the cubic phase, long-range electrostatic forces split the A_1+E modes into TO and LO components. Splitting of the B_1+E modes is also allowed; however, this has not been observed.[4–6] The B_1+E modes we designate as "silent". In this paper, we will follow the labeling scheme used by Burns and Scott,[4] namely, that the modes that arise from the $3T_{1u}$ modes are labeled in sequence 1, 2, and 3 from low to high frequency. For example, the three E(TO) modes will be called E(1TO), E(2TO), and E(3TO), and similarly for the $3E$(LO), $3A_1$(TO), and $3A_1$(LO) modes. As with the cubic (PE) phase, this description of the phonons as LO or TO in the FE phase is valid only when **k** is along one of the principal symmetry directions of the crystal.

In Figs. 1(a) and 1(b), we show the polarized Raman spectra of $PbTiO_3$ in platelet and backscattering geometries, respectively. In both scattering geometries, **k** lies in the basal plane along the principal **a** axis. From the selection rules, the three peaks observed in the platelet $\mathbf{q}\|\mathbf{a}$ (zz) polarized spectrum should correspond to the $3A_1$(TO) modes. An identical spectrum is observed in backscattering $x(zz)x$. Burns and Scott[4] observed a similar spectrum in $x(zz)y$ geometry and assigned the two higher energy peaks at 359.5 and 647.0 cm^{-1} to the A_1(2TO) and A_1(3TO) modes, respectively. However, the lowest-frequency peak at 148.5 cm^{-1} was not assigned to the A_1(1TO) phonon, but was interpreted as an "extraneous" line. This assignment was justified because strong extraneous mode peaks had previously also been observed in $BaTiO_3$.[18] While it is assumed that such modes arise from some higher-order scattering process, no detailed explanation of their origin has been proposed. In the more recent Raman study,[6] the peak at 148.5 cm^{-1} was assigned to the A_1(1TO) phonon, based on its polarization.

The Raman selection rules determine that the $x(yz)x$ backscattering geometry allows only E(TO) modes, while both E(TO) and E(LO) modes are allowed in the platelet geometry $\mathbf{q}\|\mathbf{a}$ $(zx)+(zy)$ polarization. We therefore assign the peaks at 87.5, 218.5, and 505.0 cm^{-1} to the E(1TO), E(2TO), and E(3TO) phonons, respectively, and the peaks at 128.0, 440.5, and 687.0 cm^{-1} to the E(1LO), E(2LO), and E(3LO) phonons, respectively. These assignments confirm those of Ref. 4 with the exception of the E(3LO), which was not observed by Burns and Scott. The measured frequency of this mode is ≈ 36 cm^{-1} lower than the fitted value in Ref. 4. The peak at 289 cm^{-1} is assigned to the E-symmetry component of the silent mode.

For platelet $\mathbf{q}\|\mathbf{a}$ $(xx)+(yy)+(xy)$ polarized and backscattering $x(yy)x$ geometries, the only allowed phonons should be the $3A_1$(TO) modes and the B_1-symmetry component of the silent mode. Clearly the peak at 289 cm^{-1} corresponds to silent mode, while the peaks at 359.5 and 647.0 cm^{-1} correspond to the A_1(2TO) and A_1(3TO) modes, respectively. From selection rules it is tempting to assign the mode at 148.5 cm^{-1} as the A_1(1TO) mode; however, the high resolution of our data (0.5 cm^{-1}) shows that this peak exhibits an anomalous line shape unexpected for a single phonon. In previous low-resolution data (4.0 cm^{-1} for Refs. 4 and 6), the line shape only showed a slight asymmetry. In our data, this feature appears to consist of several peaks. In the next section we present data that show that this feature is indeed the A_1(1TO) phonon and identify the $3A_1$(LO)

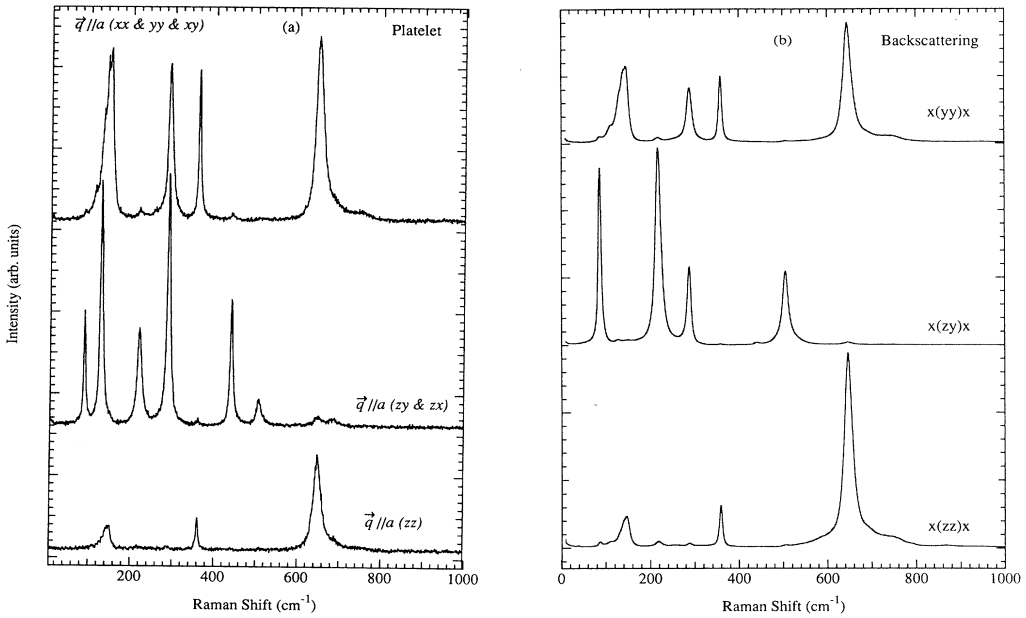

FIG. 1. Polarized Raman spectra of single-domain single-crystal $PbTiO_3$ at 300 K in (a) platelet and (b) 180° backscattering. The Raman selection rules are strictly obeyed. The bottom curves show the three A_1(TO) phonons. The middle curves show the four E(TO) modes, and the platelet $\mathbf{q}\|\mathbf{x}$ $(zx)+(zy)$ polarization curve also shows the four E(LO) modes. The top curve shows the B_1-symmetry component of the silent phonon in addition to the three A_1(TO) phonons.

modes not observed in Fig. 1. In Sec. V, we discuss and explain the anomalous line shape of the A_1(1TO) mode.

IV. OBLIQUE MODE ANGULAR DEPENDENCE

For uniaxial crystals, the phonon mode frequencies disperse as a function of the angle θ between **k** and the **c** axis (i.e., the direction of the spontaneous polarization in the FE phase). Phonons observed at $\theta=0,\pi/2$ correspond to the pure LO and TO phonons, while at intermediate values of θ, the modes are termed oblique phonons or "quasimodes." The frequency dispersion of the oblique phonons is given by the zeros of Merten's equation:[11]

$$\varepsilon_c(\omega)\cos^2\theta+\varepsilon_a(\omega)\sin^2\theta=0\ , \tag{1}$$

where $\varepsilon_c(\omega)$ and $\varepsilon_a(\omega)$ are the dielectric constants as a function of ω along the **a** and **c** axes, respectively, and θ was described previously (see Fig. 2). For $\theta=0$ or $\pi/2$, Eq. (1) gives the frequencies of the A_1 or E-symmetry LO modes, respectively [e.g., $\theta=0\Longrightarrow\varepsilon_c(\omega)=0\Longrightarrow A_1$(LO)]. We can write the dielectric constant along either of the principal axes in terms of the TO and LO frequencies as follows:[18]

$$\frac{\varepsilon_c(\omega)}{\varepsilon_c(\infty)}=\frac{\prod_i[\omega_c(i\mathrm{LO})^2-\omega^2]}{\prod_i[\omega_c(i\mathrm{TO})^2-\omega^2]}\ ,$$
$$\frac{\varepsilon_a(\omega)}{\varepsilon_a(\infty)}=\frac{\prod_i[\omega_a(i\mathrm{LO})^2-\omega^2]}{\prod_i[\omega_a(i\mathrm{TO})^2-\omega^2]}\ , \tag{2}$$

where ω_c and ω_a are the frequencies of the A_1 and E modes, respectively, and $\varepsilon_c(\infty)$ and $\varepsilon_a(\infty)$ are the dielectric constants derived from the ordinary and extraordinary refractive indices, respectively, in a frequency region that is high compared to all the lattice modes, but low compared to the electronic energies. Combining Eq. (1) with Eq. (2) yields Merten's equation:[4–11]

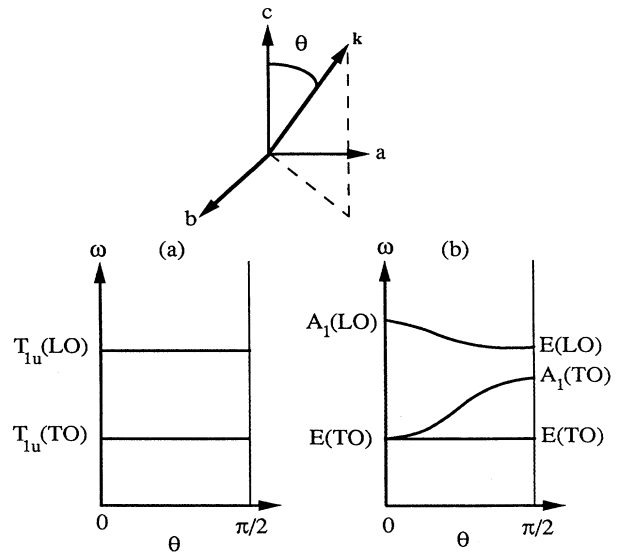

FIG. 2. Schematic of the frequency dispersion of the TO and LO phonons as a function of θ, the angle between the **c** axis and the phonon wave vector **k**, for (a) cubic O_h^1 ($Fm3m$), and (b) tetragonal C_{4v}^1 ($P4mm$) symmetry.

$$\varepsilon_c(\infty)\cos^2\theta \prod_i [\omega_c(i\mathrm{LO})^2-\omega^2] \prod_i [\omega_a(i\mathrm{TO})^2-\omega^2]+\varepsilon_a(\infty)\sin^2\theta \prod_i [\omega_a(i\mathrm{LO})^2-\omega^2] \prod_i [\omega_c(i\mathrm{TO})^2-\omega^2]=0 . \quad (3)$$

If the frequencies of all the $3n-3$ optical phonons along the principal axes are known, then the frequencies of the oblique modes of the crystal at any angle θ are given by the $3n-3$ values of ω which satisfy Eq. (3). In Figs. 2(a) and 2(b), we schematically depict the angular dispersion behavior of the oblique phonons for both cubic and uniaxial crystals, respectively. It is important to note that the group symmetry labels for **k** along the principal axes in Fig. 2 are only suggested since the solutions to Eq. (3) do not specify the symmetry of the modes. The actual symmetries will depend on whether the elastic anisotropy is larger or smaller than the electrostatic splitting.[11]

Figure 3(a) shows the unpolarized Raman spectra of $PbTiO_3$ obtained in platelet geometry. This geometry permits mapping of the entire angular dependence of the oblique phonon modes of the material.[17] The spectra in Fig. 3(a) give the frequencies of the oblique phonons for specific directions of **k** corresponding to various values of θ. Along the principal direction **k**||**c**, we observe peaks at 194.0, 465.0, and 795.0 cm^{-1}, in addition to the previously assigned $3E$(TO) modes and the silent mode. We assign these peaks to the A_1(1LO), A_1(2LO), and A_1(3LO) modes, respectively. Burns and Scott[4] reported the A_1(2LO) mode at 440.5 cm^{-1}, degenerate with the E(2LO) mode, about 24.5 cm^{-1} lower than our observed value. The weak A_1(1LO) mode was not directly observed by Burns and Scott,[4] but can easily be identified from the oblique mode spectra in Fig. 3(a). The frequency of the A_1(1LO) mode in Ref. 4 was determined to be 215 cm^{-1} by fitting to Merten's relation, approximately 21.0 cm^{-1} higher than our measured value.

From the Raman spectra in Fig. 3(a), the angular dependence of the peak positions is clearly shown. The peak at 440.5 cm^{-1} and the shoulder at 687.0 cm^{-1} (**k**||**a**), which we identified as the E(2LO) and E(3LO), respectively, disperse upward to 465.0 and 795.0 cm^{-1} to become the A_1(2LO) and A_1(3LO) modes (**k**||**c**), respectively. The A_1(3TO) mode at 647.0 cm^{-1} (**k**||**a**) disperses downward to merge with the E(3TO) mode at 505.0 cm^{-1} (**k**||**c**). The A_1(3TO) mode at 359.5 cm^{-1} (**k**||**a**) disperses downward, through the silent mode peak at 289.0 cm^{-1}, showing no evidence of coupling, to merge with the E(3TO) mode at 218.5 cm^{-1} (**k**||**c**). This mode crossing is, in principle, not allowed because both modes have some E-symmetry character. However, it may be that since the 289.0 cm^{-1} mode originates from the cubic T_{2u}, whereas the 359.5 and 218.5 cm^{-1} modes arise from the cubic T_{1u}, the coupling is too small to be observed. The same mode crossing was observed in the pressure dependence of the Raman modes in $PbTiO_3$ (Ref. 7). At low frequency, the E(1LO) mode at 128.0 cm^{-1} (**k**||**a**) disperses downward to merge with the E(1TO) mode at 87.5 cm^{-1} (**k**||**c**).

The polarized platelet **q**||**a** (zz) data [Fig. 1(a)] as well as

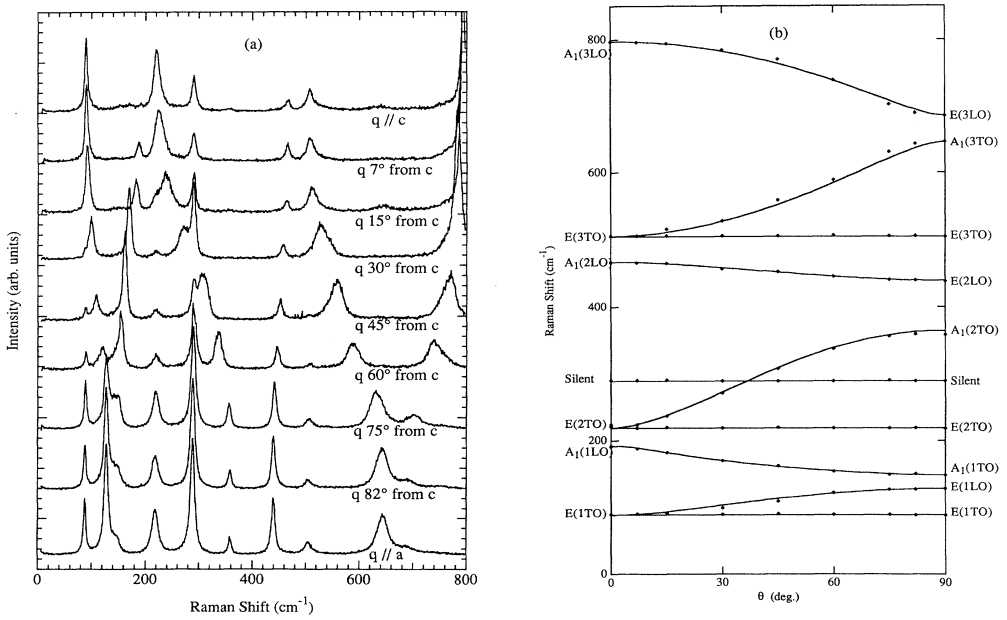

FIG. 3. (a) Raman spectra of the oblique phonons of single-domain single-crystal $PbTiO_3$ at 300 K in platelet geometry for various directions of the phonon wave vector **k**. Frequencies of the oblique phonons (♦) in $PbTiO_3$ are plotted as a function of θ, the angle between the **c** axis and the phonon wave vector **k**. The solid lines are the predicted angular frequency dispersion curves derived from Merten's equation, Eq. (3), using the principal axes frequencies shown in Table I. The principal axes symmetries were derived from the Raman selection rules (see Fig. 1).

the backscattering $x(zz)x$ data [Fig. 1(b)] indicates that the shoulder observed in Fig. 3(a) at 148.5 cm^{-1} for $\mathbf{k}\|\mathbf{a}$ obeys the Raman selection rules for A_1(TO) symmetry. In addition, this peak exhibits an anomalous line shape for $\mathbf{k}\|\mathbf{a}$. As this peak disperses upward, the asymmetry of the line shape decreases. By $\theta=60°$, the line-shape asymmetry has significantly diminished, and by $\theta=45°$, the line shape appears essentially symmetric as was reported in Ref. 4. For $\theta<45°$, the mode continues to disperse upwards, connecting to the A_1(1LO) mode at 194.0 cm^{-1} ($\mathbf{k}\|\mathbf{c}$), with an associated dramatic decrease in peak intensity. It is important to note that this peak does not correspond to the weak second-order Raman spectrum of $PbTiO_3$ reported in Ref. 6. Since the angular dispersion data in Fig. 3(a) connect the 148.5 cm^{-1} peak to the A_1(1LO) mode, we conclude that the 148.5 cm^{-1} peak is a fundamental phonon that exhibits an anomalous line shape. The assignment of this peak to the A_1(1TO) mode is natural since this satisfies the Raman selection rules and since this is the only remaining unassigned phonon.

The data in Figs. 1 and 3(a) are summarized in Table I, which lists the frequencies and symmetry assignments for the zone-center optical phonons in $PbTiO_3$ at room temperature. In Fig. 3(b), the frequency values (♦) of the oblique phonon modes in $PbTiO_3$ are plotted versus θ, and the symmetry assignments established from the data are labeled along the principal axes. The frequencies of the pure TO and LO phonons listed in Table I, together with the literature values[19] of ε_a and ε_c were used to calculate the solutions to Merten's relation, Eq. (3). The resulting dispersion curves are shown as solid lines in Fig. 3(b). The largest discrepancy between the frequencies predicted by Merten's relation and the measured angular dependence of the quasimode frequencies is ≈ 8 cm^{-1}. The close agreement between Merten's relation and the data further substantiates the assignment of the A_1(1TO) mode to the asymmetric peak at 148.5 cm^{-1}.

The complete angular dependence shown in Fig. 3(b) also allows us to understand the differences between the present work and that of Ref. 4. From quasimode frequencies at $\theta=45°$, together with the subset of principal-axes mode frequencies which they could measure, Burns and Scott[4] used a trial and error method of fitting to Merten's relation to determine the frequencies of the A_1(1TO), A_1(1LO), and E(1LO) modes (which were not observed). However, they reported the frequency of the A_1(2LO) degenerate with the E(2LO) mode. Since the solutions of Merten's equation depend on the frequencies of all the principal-axes modes, any error in the frequencies of these modes will effect the accuracy of the quasimode dispersions. Therefore, the frequencies of any unknown principal-axes modes which are being fitted will be erroneous. Given the trial and error method of fitting employed by Burns and Scott,[4] their results were remarkably accurate. In the present work, all principal-axes modes were directly measured. Therefore, the dispersion curves which we obtained from Merten's relation [see Fig. 3(b)] were determined using no adjustable parameters.

From Table I, we note that at $T=300$ K the frequency of the A_1(1TO) mode is higher than the frequency of the E(1LO) mode. The frequency of the A_1(1TO) mode is predicted to exhibit soft-mode behavior; whereas, the frequency of the E(1LO) mode should be relatively insensitive to temperature. In Ref. 4, the soft-mode behavior of the A_1(1TO) mode in $PbTiO_3$ was measured by observing the softening of the oblique phonon measured at 106 cm^{-1} ($T=300$ K) for $\theta=45°$. The data in Fig. 3 indicate that this quasimode is associated with the E(1LO) phonon for $T=300$ K and not the A_1(1TO) phonon. This implies that at some elevated temperature, the energies of the E(1LO) and A_1(1TO) $\mathbf{k}\cong\mathbf{0}$ modes must cross, and the soft oblique phonon associated with the E(1LO) phonon (at 300 K) will then connect the E(1TO) and the A_1(1TO) phonons. The soft-mode behavior reported in Ref. 4 qualitatively shows that the majority of the mode softening occurs within 50 K of T_c. Therefore, it is possible that the E(1LO)–A_1(1TO) mode crossing could occur in the vicinity of T_c and play a role in the dynamics of the phase transition. The soft-mode behavior of the A_1(1TO) mode reported in Ref. 6 does track the softening of the 148.5 cm^{-1} peak. Significant softening was reported, indicating that a mode crossing should occur at ≈ 700 K; however, the complex nature of the line shape of this mode was not addressed. We are currently extending our studies of the Raman modes of $PbTiO_3$ to higher temperatures in order to investigate the A_1(1TO) phonon softening and the anticipated mode crossing.

From the frequencies in Table I, we calculate the clamped dielectric constants along the **a** and **c** axes in the Raman frequency region by considering the $\omega=0$ limit of Eq. (2). This limit results in the generalized form of the LST relationships[20,21] which is appropriate for anisotropic systems in which more than one phonon contributes to the dielectric constant. Using the ordinary and extraordinary refractive indices at a wavelength of 1.0 μm, viz. $\varepsilon_c(\infty)=6.6419$ and $\varepsilon_a(\infty)=6.6301$ (Ref. 19), the clamped dielectric constants at 300 K derived from Eq. 4 are $\varepsilon_c(0)=28.6$ and $\varepsilon_a(0)=106.9$. We have previously reported the anisotropic dielectric constants at constant strain for our crystals.[15] The values of $\varepsilon_c^s=34.0$ and $\varepsilon_a^s=105.0$, determined by impedance measurements at 12 MHz, compared well to the dielectric constants derived from the LST relationships. This indicates that high-frequency dielectric relaxation does not occur in $PbTiO_3$ single crystals, which is contrary to the case of $BaTiO_3$

TABLE I. Frequencies (in cm^{-1}) of the principal axis TO and LO phonons and dielectric constants (Ref. 19) used for the calculation of the quasimode frequencies using Merten's relation in $PbTiO_3$.

E(TO)	E(LO)	A_1(TO)	A_1(LO)	B_1+E
87.5	128.0	148.5	194.0	289.0
218.5	440.5	359.5	465.0	
505.0	687.0	647.0	795.0	

$\varepsilon_a(\infty)=6.6301$, $\varepsilon_c(\infty)=6.6419$

where the ε_c^s measured by the impedance method is much higher than that calculated from the LST relations.[20,21]

In Ref. 6, similar agreement between LST calculations and impedance measurements of the dielectric constants was reported between $T=300$ to 700 K. However, for $T>700$ K, a large disagreement between these two methods was observed. In addition, the Raman data showed evidence of a central mode in this same temperature region. The appearance of a central mode in the Raman scattering would appear to indicate an order–disorder component to the ferroelectric phase transition; more work is clearly needed to resolve this issue.

V. A_1(1TO) LINE SHAPE AND ANHARMONICITY

As can be discerned in Fig. 1, the A_1(1TO) mode exhibits an anomalous line shape. In Fig. 4, we show the detailed temperature dependence of the line shape of this mode taken in backscattering $x(yy)x$ geometry; the solid lines represent the experimental data. An important point to note is that the line shape is not a smooth function but appears to be a superposition of subpeaks. At $T=400$ K, the line shape clearly shows four distinct peaks at 148.5, 137.5, 126.5, and 110.5 cm^{-1}. We will label the peaks 1, 2, 3, and 4, respectively. The lowest-energy shoulder at ~ 87.5 cm^{-1} results from leakage of the strong E(1TO) mode. The relative intensities of the different data sets have been normalized. At every temperature, the strength of the E(1TO) mode leakage remained constant. It is clear from Fig. 4 that as the temperature is lowered, the intensity of peaks 2–4 decrease, and the individual peaks become more difficult to resolve. In an effort to deconvolute the line shape of the A_1(1TO) mode, we fit the spectra to a sum of Lorentzian functions.[7] The purpose of this fit was only to obtain qualitative information about the temperature dependence of the intensity of the peaks comprising the A_1(1TO) phonon line shape. The dotted lines (almost indistinguishable from the experimental data) are the result of the fit to Eq. (5) and the dashed lines are the individual Lorentzian components. By 60 K, the intensities of peaks 2–4 are so weak that the resulting line shape is essentially a single Lorentzian.

The line shapes of the experimental peaks in Fig. 4 can be qualitatively understood assuming a double-well potential for the A_1(1TO) phonon as shown in Fig. 5(a). From normal-mode calculations,[22] the ionic motions at the Γ point calculated for the A_1(1TO) phonon of $PbTiO_3$ are a relatively rigid displacement of the distorted O_6 octahedra relative to the Ti ion and the pseudocubic Pb cage; this is shown schematically in Fig. 5(b). This type of potential is eminently reasonable for tetragonal ferroelectric materials such as $PbTiO_3$ (Ref. 23), and it describes the two equivalent minima corresponding to the two equivalent states of dielectric polarization (i.e., $+z$ and $-z$); it is known[24] that the anharmonic contributions to the lattice potential energy are so large that they cannot be treated in perturbation theory. The explanation we propose is that the low-frequency shoulders of the A_1(TO) mode are due to transitions between the excited

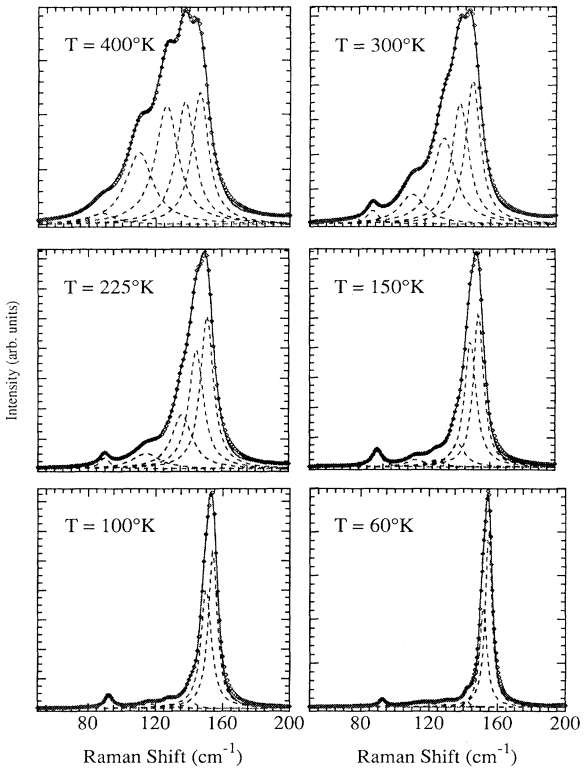

FIG. 4. Temperature dependence of the line shape of the A_1(1TO) phonon obtained in 180° backscattering. The solid line represents the experimental data and the dotted line is the result of a fit to a sum of Lorentzian functions and the dashed lines are the individual Lorentzian components.

phonon states in the potential well. We illustrate these transitions in Fig. 5(a), where the energy levels shown in one side of the double well depict the possible phonon states associated with the A_1(1TO) mode. Peak 1 of this phonon (highest energy) would correspond to a transition from the first excited state to the ground state (Stokes scattering). Peaks 2–4 would correspond to transitions from higher-energy excited states to adjacent lower-energy excited states. It should be emphasized that this is not a two-phonon process since it only involves a single quantum. This distinction of transitions between the different levels of the potential arises as a direct result of the lifting of the degeneracy of the transitions in the harmonic approximation.[25]

The arguments of the preceding paragraph can be made more rigorous in the following way: consider the potential energy $\Phi(Q)$ for the normal-mode coordinate Q of the form[24]

$$\Phi(Q)=\frac{\tilde{k}_s}{2}Q^2+\frac{\xi}{4}Q^4+\frac{\zeta}{6}Q^6 . \tag{4}$$

This potential, schematically shown in Fig. 5(a), can be envisioned either in the extended mode representation (phonon picture) or as a local normal coordinate.[25–27] In this latter case it qualitatively corresponds to the atomic motion depicted in Fig. 2(b). By applying perturbation theory to one of the anharmonic minimums of the

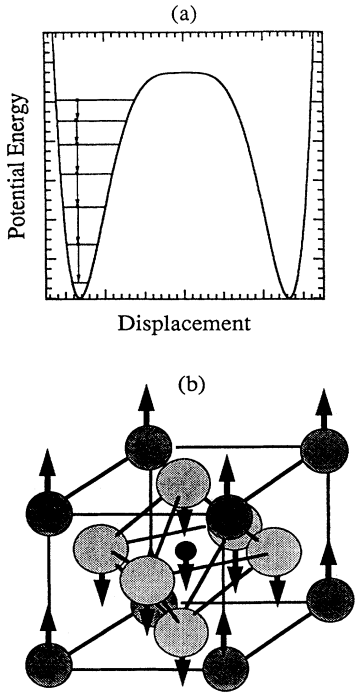

FIG. 5. (a) Schematic representation of the double-well potential along the c axis in the ferroelectric phase of $PbTiO_3$, illustrating the anharmonic nature of the potential of the A_1(1TO) phonon. We attribute the complex nature of the line shape of this mode to transitions between the excited phonon states in the well. (b) An illustration of the atomic displacements associated with the A_1(1TO) phonon for $\mathbf{k}\cong\mathbf{0}$.

double-well potential, the calculation of the energy levels can be performed in either representation. In the extended picture the result has the same form as the partial anharmonic contribution to the free energy.[28] In the local picture one can directly use the more familiar equations for anharmonic corrections from Ref. 29. Both approaches lead to energy differences between levels $E_{n+1}-E_n$ of the form,

$$\Delta E = E_{n+1}-E_n = \hbar\omega_0 - f(\tilde{k}_s,\xi,\zeta,n)\ , \tag{5}$$

where $\hbar\omega_0$ is the solution to the harmonic part of Eq. 4 and f is a function which depends on the parameters $\tilde{k}_s$, ξ, ζ, and n. To lowest order, the correction term f in Eq. 5 is linear in n (Ref. 29) leading to an expected splitting between our measured subpeaks, which is independent of n. From our 400 K data, we find that the spacings between subpeaks are 11, 12, and 15 cm^{-1}; that these spacings are not equal is attributed to higher-order perturbation corrections.

Since the intensity of a given transition is proportional to the population of the initial state which is determined from the Gibbs distribution[29] and, in the harmonic approximation, the matrix element is proportional to $\sqrt{n+1}$ (Ref. 30), the relative intensity R of the transition (Stokes) from level $n+1$ to n to that of the 1 to 0 transition is given by

$$R = (n+1)\exp\left[-\frac{n\hbar\omega}{k_bT}\right]\ , \tag{6}$$

where for the phonon in question $\hbar\omega$ is 148 cm^{-1} = 213 K and k_b is Boltzman's constant. In Table II, we list the intensity ratio values determined from Eq. 6 at various temperatures and compare them with the integrated intensities of the A_1(1TO) phonon subpeaks 1 through 4 obtained from the fit to the Raman data (see Fig. 4). Above 200 K the agreement is excellent; below this temperature the agreement is less good but the observed discrepancies can be traced to the difficulty in obtaining reliable intensities of the weak subpeaks.

An additional consequence of our interpretation is that the high-lying phonon states in the well should also have shorter lifetimes so that we expect the peak linewidths to gradually broaden as the energies of the levels increase. This is also qualitatively observed in the line shapes in Fig. 4; however, due to problems of deconvoluting the instrumental resolution from the fitted linewidths we are unable to claim more than just qualitative agreement.

Recently, Raman line shapes composed of multiple peaks have been reported in the coherent anti-Stokes Raman-scattering vibron spectrum of shock compressed N_2 (Ref. 31) (i.e., $T>2500$ K and pressure >10 GPa). In this report, the nature of the line shape was associated with the anharmonic component of the molecular potential in the molecular crystal. The current article is a re-

TABLE II. Theoretical and experimental intensity ratios of the peaks associated with the A_1(1TO) phonon line shape.

Temperature	60 K	100 K	150 K	225 K	300 K	400 K
			Theory			
0 to 1	1.00	1.00	1.00	1.00	1.00	1.00
1 to 2	0.057	0.23	0.48	0.78	0.98	1.17
2 to 3	0.002	0.04	0.18	0.45	0.73	1.03
3 to 4		0.01	0.06	0.23	0.48	0.81
			Experiment			
0 to 1	1.00	1.00	1.00	1.00	1.00	1.00
1 to 2	0.62	0.81	0.84	0.88	0.98	1.22
2 to 3	0.02	0.05	0.22	0.55	0.87	1.04
3 to 4	0.01	0.05	0.08	0.21	0.35	0.87

port of anharmonicity-associated multiple-peak Raman line shapes in the phonon spectrum of a solid under conditions of temperature and pressure near ambient.

VI. CONCLUSION

We have reported detailed Raman studies of the optical phonons of high-quality single-crystal $PbTiO_3$. All $\mathbf{k} \cong \mathbf{0}$ optical-phonon modes are directly observed and are shown to obey rigorously Raman selection rules indicating that the mode energies and symmetry assignments in the literature[4] must be revised. The angular dependence of the oblique phonon frequencies was shown to compare well with the predicted dispersion from Merten's relation. We showed that the energy of the lowest-frequency A_1(TO) mode is higher than the energy of the lowest-frequency E(LO) mode at 300 K indicating that these two $\mathbf{k} \cong \mathbf{0}$ modes will cross at elevated temperature. We have proposed a model in which we attribute the anomalous line shape of the A_1(TO) mode to the anharmonic nature of the lattice. The phonon frequencies determine the clamped dielectric constants, $\varepsilon_a(0)$ and $\varepsilon_c(0)$, using the Lydanne-Sachs-Teller relation. These values, when compared to those obtained from impedance measurements, indicate no dielectric dispersion in $PbTiO_3$ between the MHz region and the Raman region.

ACKNOWLEDGMENTS

We would like to thank Dr. X.-Z. Xu for the growth of the $PbTiO_3$ single crystals. This work has been supported by the U.S. Department of Energy, Basic Energy Sciences-Materials Sciences under Contract No. W-31-109-ENG-38.

[1]F. Jona and G. Shirane, *Ferroelectric Crystals* (Pergamon, New York, 1962).
[2]G. Shirane, J. D. Axe, and J. Harada, Phys. Rev. B **2**, 155 (1970).
[3]C. H. Perry and B. N. Kanna, Phys. Rev. **135**, A408 (1964).
[4]G. Burns and B. A. Scott, Phys. Rev. Lett. **25**, 167 (1970); Phys. Rev. B **7**, 3088 (1973).
[5]N. E. Tornberg and C. H. Perry, J. Chem. Phys. **53**, 1946 (1970); G. Burns, Phys. Rev. Lett. **37**, 229 (1976).
[6]M. D. Fontana, H. Idrissi, G. E. Kugel, and K. Wojcik, Ferroelectrics **80**, 117 (1988); M. D. Fontana, H. Idrissi, G. E. Kugel, and K. Wojcik, J. Phys. Condens. Matter **3**, 8695 (1991).
[7]F. Cerdeira, W. B. Holzapfel, and D. Bäuerle, Phys. Rev. B **11**, 1188 (1975); J. A. Sanjurjo, E. López-Cruz, and G. Burns, *ibid.* **28**, 7260 (1983).
[8]J. Feder and E. Pytte, Phys. Rev. B **1**, 4803 (1970).
[9]N. S. Gillis and T. R. Koehler, Phys. Rev. B **5**, 1925 (1972).
[10]E. Pytte, Phys. Rev. B **5**, 3758 (1972).
[11]R. Loudon, Adv. Phys. **13**, 413 (1964); L. Merten, Phys. Status Solidi **25**, 125 (1968).
[12]Z. Li, X. Z. Xu, X. H. Dai, D. J. Lam, and S.-K. Chan, in *Ceramics-Adding the Value,* edited by M. J. Bannister (CSIRO, Melbourne, Australia, 1992), Vol. 1, pp. 457–462.
[13]J. P. Remeika and A. M. Glass, Mater. Res. Bull. **5**, 37 (1970).
[14]Z. Li, C. M. Foster, X.-Z. Xu, S.-K. Cha-n, and D. J. Lam, J. Appl. Phys. **71**, 4481 (1992).
[15]X. H. Dai, Z. Li, X. Z. Xu, S.-K. Chan, a . J. Lam, Ferroelectrics **135**, 39 (1992).
[16]K. Wojcik, Ferroelectrics **99**, 5 (1989).
[17]M. Grimsditch, Physica B **150**, 271 (1988).
[18]A. Pinczuk, E. Burnstein, and S. Ushioda, Solid State Commun. **7**, 139 (1969); G. Burns and B. A. Scott, *ibid.* **9**, 813 (1971).
[19]S. Singh, in *Handbook of Laser Science and Technology,* edited by Marvin J. Weber (CRC Boca Raton, FL, 1986), Vol. 3, Part 1, p. 158.
[20]Z. Li, S.-K. Chan, M. H. Grimsditch, and E. S. Zouboulis, J. Appl. Phys. **70**, 7327 (1991).
[21]A. Scalabrin, A. S. Chaves, D. S. Shim, and S. P. S. Porto, Phys. Status Solidi B **79**, 731 (1977).
[22]J. D. Freire and R. S. Katiyar, Phys. Rev. B **37**, 2074 (1988).
[23]A. D. Bruce, K. A. Müller, and W. Berlinger, Phys. Rev. Lett. **42**, 185 (1979).
[24]T. Hidaka, J. Phys. Soc. Jpn. **61**, 1054 (1992).
[25]C. M. Foster, M. Grimsditch, Z. Li, and V. G. Karpov (unpublished).
[26]R. J. Elliot, J. Phys. C **4**, L179 (1971).
[27]M. A. Moore and H. C. W. L. Williams, J. Phys. C **5**, 3185 (1972).
[28]See, for example, G. Leibfried and W. Ludwig, in *Solid State Physics,* edited by F. Seitz and D. Turnbull (Academic, New York, 1961), Vol. 12, p. 275, in particular Eqs. 10.2 through 10.4.
[29]L. D. Landau and E. M. Liftshitz, *Statistical Physics* (Pergamon, London, 1959).
[30]L. D. Landau and E. M. Liftshitz, *Quantum Mechanics, Non-Relativistic Theory* (Pergamon, London, 1959).
[31]D. Schiferl, R. LeSar, and D. S. Moore, in *Simple Molecular Systems at Very High Density,* edited by A. Polian, P. Loubeyre, and N. Boccara (Plenum, New York, 1990), p. 303; S. C. Schmidt, D. S. Moore, and M. S. Shaw, Phys. Rev. B **35**, 493 (1987).